The Plant Cell, Vol. 27: 1512–1528, May 2015, www.plantcell.org

Role of Aminoalcoholphosphotransferases 1 and 2 in Phospholipid Homeostasis in Arabidopsis

Yu Liu,[a,b] Geliang Wang,[a,b] and Xuemin Wang[a,b,1]

[a] Department of Biology, University of Missouri, St. Louis, Missouri 63121
[b] Donald Danforth Plant Science Center, St. Louis, Missouri 63132

ORCID IDs: 0000-0002-8813-9511 (Y.L.); 0000-0002-6251-6745 (X.W.)

Aminoalcoholphosphotransferase (AAPT) catalyzes the synthesis of phosphatidylcholine (PC) and phosphotidylethanolamine (PE), which are the most prevalent membrane phospholipids in all eukaryotic cells. Here, we show that suppression of *AAPTs* results in extensive membrane phospholipid remodeling in *Arabidopsis thaliana*. Double knockout (KO) mutants that are hemizygous for either *aapt1* or *aapt2* display impaired pollen and seed development, leading to embryotic lethality of the double KO plants, whereas *aapt1* or *aapt2* single KO plants show no overt phenotypic alterations. The growth rate and seed yield of *AAPT* RNA interference (RNAi) plants are greatly reduced. Lipid profiling shows decreased total galactolipid and phospholipid content in *aapt1*-containing mutants, including *aapt1*, *aapt1*/*aapt1 aapt2*/*AAPT2*, *aapt1*/*AAPT1 aapt2*/*aapt2*, and *AAPT* RNAi plants. The level of PC in leaves was unchanged, whereas that of PE was reduced in all *AAPT*-deficient plants, except *aapt2* KO. However, the acyl species of PC was altered, with increased levels of C34 species and decreased C36 species. Conversely, the levels of PE and phosphatidylinositol were decreased in C34 species. In seeds, all *AAPT*-deficient plants, including *aapt2* KO, displayed a decrease in PE. The data show that *AAPT1* and *AAPT2* are essential to plant vegetative growth and reproduction and have overlapping functions but that AAPT1 contributes more than AAPT2 to PC production in vegetative tissues. The opposite changes in molecular species between PC and PE and unchanged PC level indicate the existence of additional pathways that maintain homeostatic levels of PC, which are crucial for the survival and proper development of plants.

INTRODUCTION

Phosphatidylcholine (PC) and phosphatidylethanolamine (PE) are two major classes of phospholipids in all eukaryotic membranes. PC, a class of bilayer forming lipid, makes up a high proportion of the glycerolipids in the outer leaflet of the plasma membrane, whereas PE is concentrated in the inner leaflet of the plasma membrane. PC and PE are also precursors to lipid mediators, such as phosphatidic acid (PA) and diacylglycerol (DAG) (Wang et al., 2006; Testerink and Munnik, 2011). PC also plays an important role in the synthesis of triacylglycerols (Chapman and Ohlrogge, 2012). In eukaryotes, PC may be produced through three known pathways: the Kennedy pathway, where DAG acquires an activated head group (CDP-choline) to produce PC; a methylation pathway, in which PC is produced from PE by three methylation steps; and a base-exchange pathway, where PC is produced from other phospholipids, such as phosphatidylserine (PS) by replacing the head group with free choline. Similarly, PE can be produced through the Kennedy pathway from DAG and CDP-ethanolamine or through a base-exchange pathway. In addition, PE can be produced from PS by decarboxylation. Other phospholipids, including PS, phosphatidylinositol (PI), and phosphatidylglycerol (PG), are generally produced through the CDP-DAG pathway, in which DAG is first activated by CTP to form CDP-DAG followed by the acquisition of free head groups (Ohlrogge and Browse, 1995). In animal cells, the Kennedy pathway is the major source of PC and PE production and the CDP-DAG pathway also contributes to the PC and PE pool in certain mammalian tissues (Noga and Vance, 2003), while the base-exchange pathway is generally regarded as a minor pathway and the direction of this reaction is toward PS production (Vance, 2008).

In plants, unique properties have been reported beyond the general pathways of phospholipid biosynthesis. First, the activity of the first methylation step of PE cannot be detected in most plant species, including *Arabidopsis thaliana* (Keogh et al., 2009). Instead, the methylation of ethanolamine was reported at the phosphoethanolamine (P-Eth) level by the enzyme P-Eth *N*-methyltransferase (PEAMT) to produce phosphomonomethylethanolamine, phosphodimethylethanolamine, and phosphocholine successively (Bolognese and McGraw, 2000). The methylated P-Eth species then enter the last two steps of the Kennedy pathway, and partially methylated head groups can be fully methylated by phospholipid *N*-methyltransferase to produce PC as the final product (Keogh et al., 2009). Second, the plant enzyme that functions at the last step of the Kennedy pathway, namely, aminoalcoholphosphotransferase (AAPT), can use both CDP-choline and CDP-ethanolamine as substrates (Goode and Dewey, 1999). By comparison, in yeast, cholinephosphotransferase 1 (CPT1) produces PC almost exclusively, while ethanolaminephosphotransferase 1 (EPT1) is bifunctional, producing PC and PE (Carman and Henry, 2007). In addition, plants produce glycerolipids in the endoplasmic reticulum (ER) and plastids, referred to as the eukaryotic pathway and prokaryotic pathway, respectively (Browse et al., 1986; Ohlrogge and Browse, 1995). These two pathways produce different subsets of glycerolipids; however, crosstalk between these two pathways has been reported (Browse et al., 1986; Ohlrogge and Browse, 1995; Wang and Benning, 2012).

[1] Address correspondence to swang@danforthcenter.org.
The author responsible for distribution of materials integral to the findings presented in this article in accordance with the policy described in the Instructions for Authors (www.plantcell.org) is: Xuemin Wang (swang@danforthcenter.org).
www.plantcell.org/cgi/doi/10.1105/tpc.15.00180

Based on the current knowledge, the Kennedy pathway plays a more prominent role than the CDP-DAG-coupled methylation pathway in PC biosynthesis in plants. The plant head group methylation pathway also depends on AAPT to produce PC. Arabidopsis has two genes, *AAPT1* and *AAPT2*, that encode enzymes with both CPT and EPT activity in vitro. Whereas both AAPTs have higher CPT activity than EPT activity, AAPT2 has even higher CPT activity than does AAPT1 (Goode and Dewey, 1999). These enzymes are able to use DAG and CDP-amino alcohols (including ethanolamine, monomethylethanolamine, dimethylethanolamine, and choline) as substrates in vitro to produce PE and PC as final products (Keogh et al., 2009), but the contributions of AAPT1 and AAPT2 to lipid metabolism in plants have not been directly tested. Here, we determined the role of *AAPTs* in plant lipid metabolism, growth, and development.

RESULTS

Mutants *aapt1* and *aapt2* Differ in Lipid Alterations

Arabidopsis AAPT1 and AAPT2 are 88% identical in amino acid sequences and share ~30% sequence identity with yeast and mammalian CPT and EPT. Both AAPTs are predicted to possess eight transmembrane domains. The AAPTs, CPTs, and EPTs from animals and yeast all share a highly conserved region, which is predicted to localize on membrane surfaces (Supplemental Figure 1), by TMHMM 2.0 (http://www.cbs.dtu.dk/services/TMHMM/). Since this conserved region is the only long, exposed peptide in AAPT protein, it is possible that it is responsible for substrate binding and catalytic activity, as shown in a recent structural analysis of CDP-alcohol phosphotransferase (Sciara et al., 2014). Both *AAPTs* were expressed in young vegetative tissue (Goode and Dewey, 1999). Quantitative real-time PCR (qPCR) analysis showed that *AAPT1* was expressed ~2-fold higher than *AAPT2* in rosette leaves, while *AAPT2* expression level is slightly higher than *AAPT1* in maturing seeds (Figure 1A), consistent with the microarray and RNA-seq data. Data from the Arabidopsis eFP browser (http://bar.utoronto.ca/efp/cgi-bin/efpWeb.cgi) indicate that *AAPT1* is expressed in almost all plant tissues, while *AAPT2* expression level is lower than *AAPT1* in vegetative rosette leaves and higher in maturing seeds and pollen. Data from Genevestigator (https://www.genevestigator.com/gv/plant.jsp) show that both *AAPT1* and *AAPT2* are highly upregulated in sperm cells (Supplemental Figures 2A and 2B), indicating they may have important functions in male gamete development.

T-DNA insertional lines were isolated for *AAPT1* (*aapt1-1*; SALK_059178) and *AAPT2* (*aapt2-1*; SALK_150255). The insertion site of *aapt1-1* is in the 14th exon, while that of *aapt2-1* is in the first exon (Figure 1B). Homozygous lines of *aapt1-1* and *aapt2-1* were identified by PCR. In addition, we attempted to generate *aapt1 aapt2* double knockout (KO) plants by crossing *aapt1-1* and *aapt2-1* homozygous lines. To test if these insertions disrupt the expression of *AAPT1* and *AAPT2* genes, qPCR was performed using wild-type, *aapt1-1*, *aapt2-1*, and both hemizygous (*aapt1/aapt1 aapt2/AAPT2* and *aapt1/AAPT1 aapt2/aapt2*) plants produced via crosses between *aapt1-1* and *aapt2-1*. Both *aapt1* and *aapt2* homozygous mutants have greatly reduced *AAPT1* and *AAPT2* transcript levels, respectively (Figure 1C).

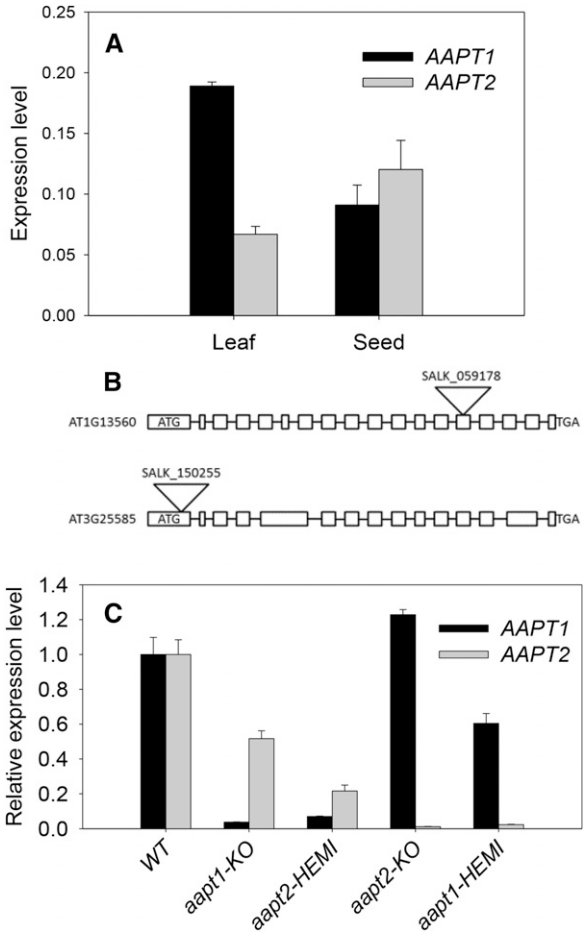

Figure 1. Expression of *AAPT1* and *2* and T-DNA Insertion Mutants of *AAPT1* and *2*.

(A) Tissue-specific expression profile of *AAPT1* and *AAPT2*. The expression level was quantified by qPCR and normalized with *UBQ10*. Values are means ± SD (n = 3).

(B) Gene structure of *AAPT1* and *AAPT2* and SALK T-DNA insertion sites. Boxes represent exons and lines represent introns.

(C) Expression of *AAPT1* and *AAPT2* in T-DNA insertion lines. RNA from leaves of *aapt1* KO, *aapt2* KO homozygotes, and *aapt1/2* hemizygotes was used for qPCR. All expression data were normalized to the wild type. Values are means ± SD (n = 3). In all figures, *aapt1-HEMI* refers to *aapt1/AAPT1 aapt2/aapt2*, and *aapt2-HEMI* refers to *aapt1/aapt1 aapt2/AAPT2*.

To explore the metabolic consequence of the KO of *AAPT* genes in plants, polar lipids from rosette leaves of wild-type, *aapt1-1*, *aapt2-1*, and hemizygous plants were quantitatively profiled. Compared with the wild type, *aapt1-1* and *aapt1/aapt1 aapt2/AAPT2* both displayed a decrease in total polar lipids (~15%) (Figure 2A) and phospholipids (~10%) (Supplemental Figure 3). The *aapt1-1* single mutant and both hemizygous mutants had decreased levels of PE, PI, and/or monogalactosyldiacylglycerol (Figures 2B and 2C). The magnitude of decrease is correlated with the number of *AAPT* genes being knocked out. In addition, lysophosphatidylethanolamine (lysoPE) decreased in the *aapt1-1* single KO and both hemizygotes (Figure

2C). A decrease in C36 PC occurred, but no significant change in C34 in *AAPT1* deficient mutants was seen (Figures 3A and 3B). On the other hand, the *aapt1* mutants displayed a decrease in both C34 PE and C36 PE species (Figures 3C and 3D). However, the relative amount of C34 PE decreased and C36 PE increased in *aapt1-1* and both hemizygotes, but not in *aapt2-1* (Supplemental Figure 4). When a construct harboring *AAPT1* was introduced into *aapt1-1*, the genetically complemented plants had similar levels of PC, PE, PG, and PI as the wild type (Supplemental Figure 5). The restoration by genetic complementation validates that the alteration of lipid levels results from the loss of *AAPT1* function. By comparison, the lipid level of *aapt2-1* KO plants was comparable to that of the wild type (Figure 2A; Supplemental Figure 3). These results are in agreement with the fact that *AAPT1* is expressed at higher levels than *AAPT2* in rosette leaves and suggest that AAPT1 contributes more than AAPT2 to glycerolipid production in leaves.

Double Loss of *AAPT1* and *AAPT2* Results in Defects in Pollen and Seed Development

No overt alterations in growth or seed development were observed in either *aapt1-1* or *aapt2-1* single mutants. To further probe the biological function of *AAPTs* in Arabidopsis, we crossed *aapt1-1* and *aapt2-1* homozygous lines to generate double KO plants. *AAPT1* and *AAPT2* reside on different chromosomes, so plants bearing both T-DNA insertions were readily obtained. However, after several rounds of self-crossing and screening, no homozygous *aapt1/aapt2* double mutants were obtained, but we were able to recover *AAPT1/aapt1 aapt2/aapt2* and *aapt1/aapt1 AAPT2/aapt2* hemizygous plants. These hemizygous plants, which have only one functional copy of *AAPT1* or *AAPT2*, were confirmed by genomic PCR and displayed a further decrease in transcript level of the respective gene (Figure 1C). The segregation ratios of self-pollinated hemizygous plants were abnormal. If no selection pressure exists, the segregation ratio of the *Aabb* genotype was predicted to be 1:2:1 for *AAbb:Aabb:aabb*. However, the actual segregation ratio is ~5:1:0 in the progeny of *AAPT1/aapt1 aapt2/aapt2* and 18:1:0 in that of *aapt1/aapt1 AAPT2/aapt2* (Figure 4). These segregation ratios are significantly different from the predicted ones and heavily favor wild-type *AAPT* progeny, indicating that strong selection pressure may exist against *aapt1/aapt2* double mutant male and female gametes.

Considering the highly elevated expression levels of *AAPT1* and *AAPT2* in sperm cells, we hypothesized that *AAPT* genes play an essential role in male gametes and pollen development.

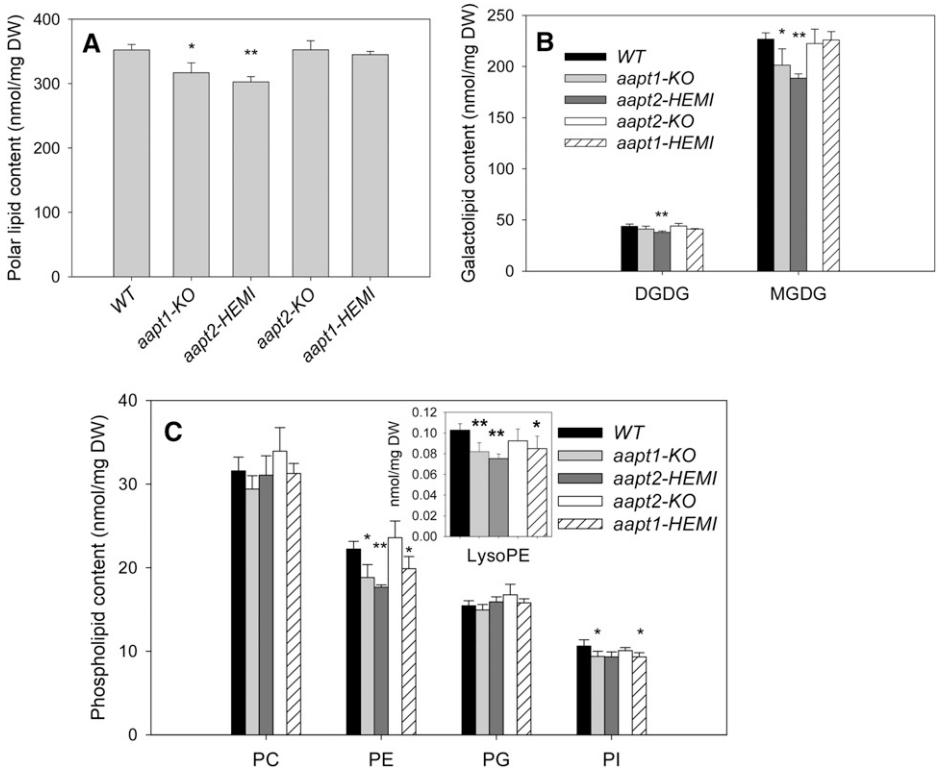

Figure 2. Changes in Phospholipids and Galactolipid Contents in *aapt* Knockout Mutants.

Polar lipids from leaves of wild-type, *aapt1/2* KO, and *aapt1/2* hemizygotes were profiled. Values are means ± SD ($n \geq 4$). Single and double asterisks mark differences between the wild type and mutant at $P < 0.05$ and at $P < 0.01$, respectively, based on Student's *t* test.

(A) Content of phospholipids and galactolipids.

(B) Galactolipid content. MGDG, monogalactosyldiacylglycerol; DGDG, digalactosyldiacylglycerol.

(C) Phospholipid content.

In all figures, *aapt1-HEMI* refers to *aapt1/AAPT1 aapt2/aapt2*, and *aapt2-HEMI* refers to *aapt1/aapt1 aapt2/AAPT2*.

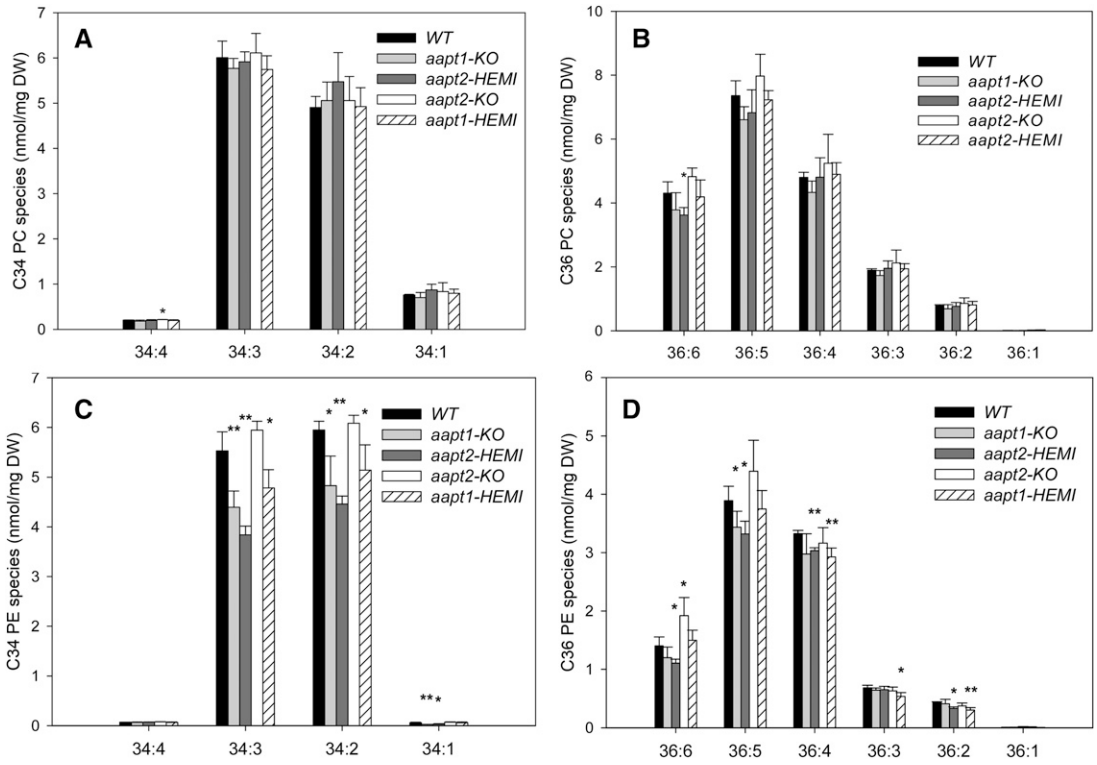

Figure 3. PC and PE Species Change.

Polar lipids from leaves of the wild type, *aapt1/2* KO, and *aapt1/2* hemizygotes were profiled. Values are means ± SD ($n \geq 4$). Single and double asterisks mark differences between the wild type and the mutant at $P < 0.05$ and at $P < 0.01$, respectively, based on Student's *t* test. **(A)** C34 PC species, **(B)** C36 PC species, **(C)** C34 PE species, and **(D)** C36 PE species. In all figures, *aapt1-HEMI* refers to *aapt1/AAPT1 aapt2/aapt2*, and *aapt2-HEMI* refers to *aapt1/aapt1 aapt2/AAPT2*.

The hemizygous plants of *aapt1* and *aapt2* may generate two types of pollen: *aapt1* or *aapt2* single mutant pollen and *aapt1 aapt2* double mutant pollen. To test whether the disruption of *AAPT1/2* affects pollen viability, anthers from the wild type, *aapt1-1*, and *aapt2-1* single mutant homozygotes, and *aapt1 aapt2* double mutant hemizygotes were detached and pollen was stained by fluorescein diacetate/propidium iodide (FDA/PI) to test for viability. More than 90% of the pollen in the wild type, *aapt1*, or *aapt2* single mutants was viable, as indicated by green fluorescein produced by active esterases (Figures 5Aa, 5Ab, 5Ad, and 5B), while ~50% of the pollen in *AAPT1/aapt1 aapt2/aapt2* and *aapt1/aapt1 AAPT2/aapt2* hemizygous lines was dead, as indicated by the red stain of propidium iodide (Figures 5Ac, 5Ae, and 5B). These data indicate that *aapt1 aapt2* double mutant pollen is not viable.

The male-sterile phenotype of *aapt1 aapt2* double mutants does not fully explain the aberrant segregation ratio in *aapt1* and *aapt2* hemizygous lines because if *a/b* double mutant male gametes are not viable, the segregation ratio of *AAbb:Aabb* would be 1:1. We then examined the maturing seeds in developing siliques of the wild type, *aapt1* or *aapt2* single mutants, and hemizygous lines. In wild-type, *aapt1*, or *aapt2* single mutant plants, seeds in siliques were green and well developed. However, both hemizygous siliques contained many aborted and underdeveloped seeds, appearing wrinkled and brown in color (Figure 5C). Combined with the pollen viability assay, these results indicate that *AAPT1* and *AAPT2* together are essential for pollen and seed development.

Suppression of Both *AAPT1* and *AAPT2* Retards Plant Growth

To further investigate the function of *AAPTs*, we suppressed *AAPT1* and *AAPT2* expression by RNA interference (RNAi). Since Arabidopsis *AAPT1* and *AAPT2* share very high nucleotide sequence identity (~87%), we used the first 500 bp of the *AAPT1* coding sequence to create a double-stranded RNA (dsRNA) construct, driven by the 35S promoter, to knockdown both genes. One major concern for dsRNA-induced RNAi is the potential off-target effects, which often lead to unpredictable and false-positive phenotypes. To confirm that our construct was designed properly, we used dsCheck (http://dsCheck.RNAi.jp/) to predict potential gene targets of our RNAi construct. The result suggests that only *AAPT1* and *AAPT2* are effective targets of our *AAPT* RNAi construct, since no perfect match and very few one and two mismatches of target nucleotides were found in several other genes, and none of them are involved in lipid metabolism (Supplemental Table 1). The *AAPT* RNAi construct was introduced into the wild-type background, and RNAi transformed plants were confirmed by qPCR. Multiple RNAi lines were isolated and three *AAPT* RNAi

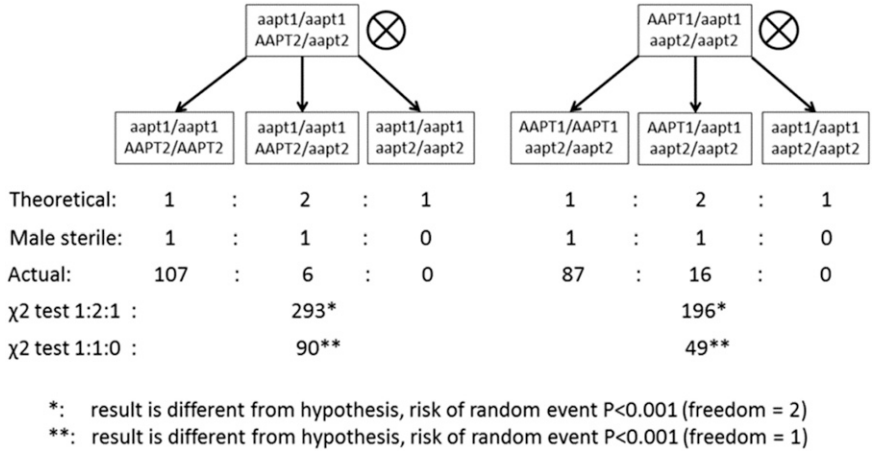

Figure 4. Segregation of *aapt* Hemizygotes.

Both hemizygotes were self-pollinated and the resulting seeds were grown and genotyped by PCR. Significance was tested based on the χ^2 test.

lines (referred to as R56, R104, and R125) with varying levels of suppression and retarded growth were used in the following studies (Figure 6A).

Two of the homozygous *AAPT* RNAi lines (R56 and R125) failed to germinate in soil. When germinated on plates, all three strong *AAPT* RNAi lines showed reduced primary root growth compared with wild-type plants (Supplemental Figure 6A). On the other hand, compared with the wild type, *AAPT* RNAi plants showed denser and longer root hairs near the root tip region (Supplemental Figures 6D and 6E). Root hair length in the elongation zone tended to be longer in RNAi plants, but root hair density in the elongation zone was comparable between wild-type and RNAi plants (Supplemental Figures 6B and 6C). By comparison, the density and length of root hair at the root tip in the *AAPT1* or *2* single KO were comparable to those of the wild type (Supplemental Figures 6D and 6E). The results suggest that deficiency of *AAPT1* or *AAPT2* does not impact the initiation and elongation of root hairs and that remodeling of the existing lipids may play a more important role. The longer and denser root hairs in the *AAPT* RNAi plants may be the result of the compensatory effect of the impaired root growth rate.

Most of these plate-germinated RNAi seedlings survived being transferred to soil; however, they continued to show smaller rosette size, smaller leaf area, and greatly reduced seed yield than the wild type (Figures 6B and 6C). The rosette size was further decreased in the homozygotes of these lines, which was evident during the segregation of the T1 generation of the R56 line (Supplemental Figure 7). To evaluate whether the severity of the phenotype is correlated with the knockdown level of *AAPT1* and *AAPT2*, transcripts of *AAPT1* and *AAPT2* in the wild-type, heterozygous, and homozygous *AAPT* RNAi plants were quantified by qPCR. The three dwarf *AAPT* RNAi lines showed a more than 80% decrease of both *AAPT1* and *AAPT2* transcript levels in rosette leaves and seeds (Figures 6D and 6E). Homozygous *AAPT* RNAi plants showed a further decrease in the transcript level for *AAPT1* and *AAPT2* (Figure 6D) compared with heterozygous RNAi plants. Collectively, these data show that the greater the decrease in *AAPT* transcript level, the greater the extent of growth inhibition in *AAPT* RNAi plants, suggesting that *AAPT* plays an essential role in the normal vegetative growth of plants.

PE, but Not PC, Is Decreased in *AAPT* RNAi Plants

We performed initial lipid profiling using wild-type and R56 heterozygous plants. There was a more than 50% decrease in PE levels and PC levels were unchanged in R56 heterozygous plants compared with the wild type. This result was validated using thin-layer chromatography (TLC) separation followed by phosphate quantification (Supplemental Figures 8A and 8B). The later isolated R104 and R125 lines further support this relationship between the knockdown of *AAPT* genes and the growth phenotype. Lipid species in rosette leaves of homozygous R56, R104, and R125 lines were profiled. Total leaf polar lipid content in R104 and R125 was comparable to that of wild-type plants but was decreased by 20% in the R56 line (Figure 7A). The total phospholipid content was decreased by 17 to 24% in all three of these lines (Figure 7B), greater than the 10% decrease in *aapt1* and *aapt1/aapt1 aapt2/AAPT2*.

When lipid classes were compared between wild-type and RNAi plants, the PC content in leaves remained unchanged in all these strong *AAPT* RNAi lines. Instead, leaf PE content was decreased by 48, 35, and 42% in the R56, R104, and R125 lines, respectively. PI and PG, which are not the direct products of the Kennedy pathway, decreased moderately (5 to 25%) in these three *AAPT* RNAi lines (Figure 7C). As for minor lipid species, lysoPE (~40%) and PA (13 to 40%) were decreased in all of these *AAPT* RNAi lines (Figure 7D), consistent with the results from *aapt1* mutants.

When lipids from seeds of wild-type, *aapt1-1*, *aapt2-1*, and *AAPT* RNAi plants were compared, PC displayed no decrease in seeds, whereas PE decreased in all mutant lines (Supplemental Figure 9). Such lipid changes are similar to those in leaves for *aapt1-1* and *AAPT* RNAi plants, but unlike those in leaves where *aapt2-1* did not impact PE levels (Supplemental Figure 9). This result is consistent with gene expression data that the transcript

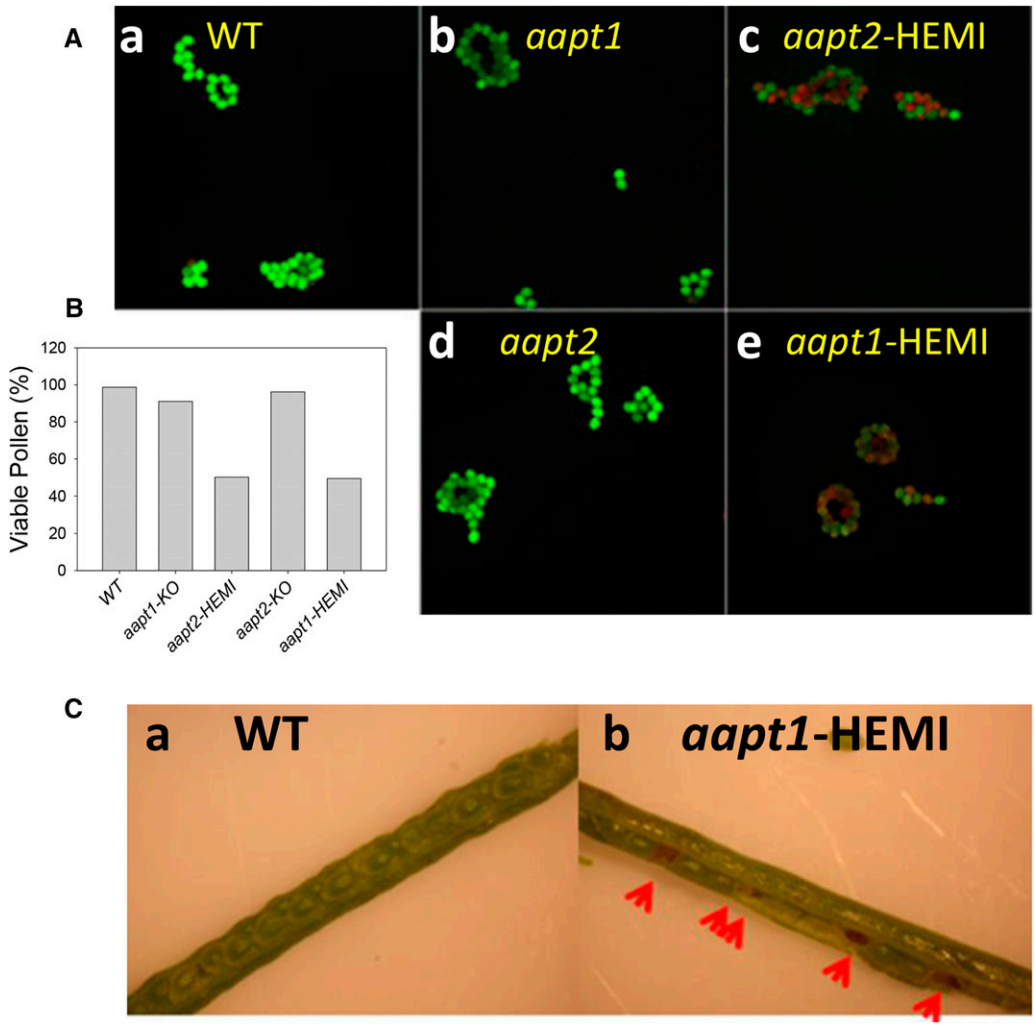

Figure 5. Defects in Pollen Viability and Seed Development in *aapt1/2* Hemizygotes.

(A) Pollen viability as indicated by FDA/PI staining. Viable pollen show green fluorescence, whereas dead pollen were stained red. **(a)** The wild type, **(b)** *aapt1* KO, **(c)** *aapt1/aapt1 AAPT2/aapt2*, **(d)** *aapt2* KO, and **(e)** *aapt1/AAPT1 aapt2/aapt2*.

(B) Percentage of viable pollen. More than 500 pollen grains from multiple anthers in each line were observed.

(C) Seed development. Siliques were peeled and observed under light microscopy. Arrows mark wrinkled or aborted seeds. **(a)** The wild type and **(b)** *aapt1/AAPT1 aapt2/aapt2.*

In all figures, *aapt1-HEMI* refers to *aapt1/AAPT1 aapt2/aapt2*, and *aapt2-HEMI* refers to *aapt1/aapt1 aapt2/AAPT2*.

level of *AAPT2* is higher in seeds than leaves (Figure 1A), suggesting that both AAPT1 and AAPT2 contribute to phosphoglycerolipid synthesis in seeds.

Inverse Changes in Molecular Species of PC and PE Species in *AAPT* RNAi Plants

Although the overall level of PC was not changed in all the *AAPT* RNAi plants, its composition of molecular species was changed significantly. In all three *AAPT* RNAi lines, the level of C36 PC species (36:5 and 36:6) was decreased by 20 to 30%, while that of C34 PC species (mainly 34:2) was increased by ~25% (Figures 8A and 8B), resulting in an unchanged total level of PC. In contrast, the relative level of PE species displayed an opposite change, with 34:3 PE species being decreased, whereas 36:5 and 36:4 PE species were increased (Figures 8C and 8D). In addition, C34 species of PI and PG were also decreased (Figures 8E and 8F).

One possibility that might explain the increased C34 PC species is the export of prokaryotic lipids, which are C34 with a C16 fatty acid at the *sn-2* position, from plastids to the ER, compensating for the loss of PC. However, lipids from the eukaryotic pathway also have a significant amount of C34 species, whereas the eukaryotic C34 PC has a C16 fatty acid at the *sn-1* position. To test the possibility, a positional analysis was used with the help of phospholipase A_2 (PLA_2) (Williams et al., 1995). We first digested total lipids from wild type and *AAPT* RNAi plants by PLA_2, which

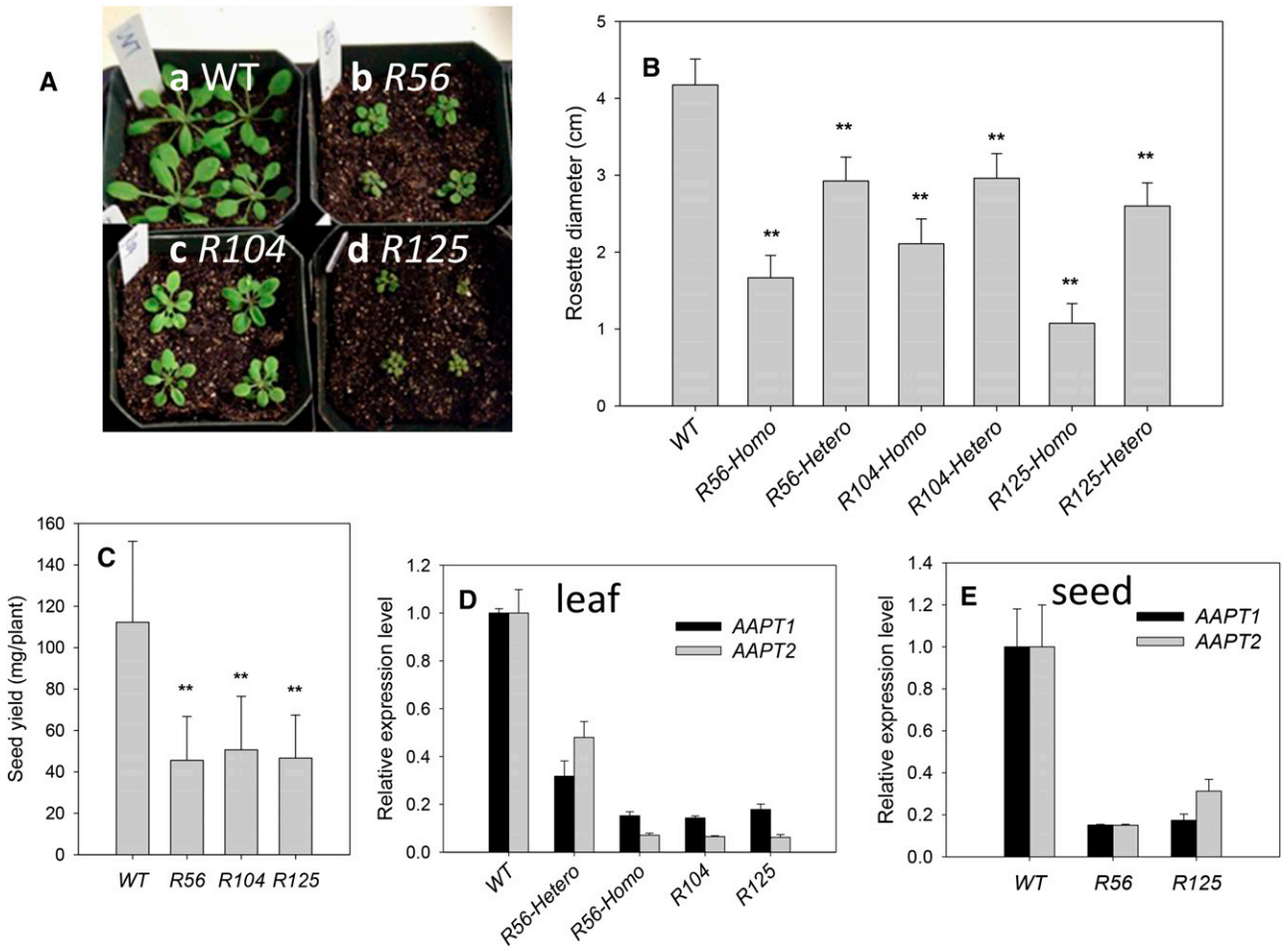

Figure 6. Effects of *AAPT* RNAi (R56, R104, and R125) on *AAPT* Expression and Plant Growth.

All plants are homozygous unless otherwise labeled.

(A) Growth phenotype of 4-week-old plants of three *AAPT* RNAi lines and the wild type.

(B) Rosette size of 4-week-old *AAPT* RNAi homozygotes (Homo), heterozygotes (Hetero), and wild-type plants. Values are means ± SD ($n \geq 10$). Asterisks indicate differences between the wild type and the mutant at $P < 0.01$ based on Student's *t* test.

(C) Seed yield of wild-type and *AAPT* RNAi homozygous plants. Values are means ± SD ($n \geq 10$). Asterisks indicate differences between the wild type and the mutant at $P < 0.01$ based on Student's *t* test.

(D) *AAPT1* and *AAPT2* expression level in leaves of *AAPT* RNAi heterozygotes (Hetero) and homozygotes (Homo). Values are means ± SD ($n = 3$).

(E) *AAPT1* and *AAPT2* expression level in seeds of wild-type and *AAPT* RNAi plants. Values are means ± SD ($n = 3$).

hydrolyzes acyl chains at the *sn-2* position of phospholipids, followed by lipid profiling to analyze lyso-phospholipid composition. The results showed that the increase of C34 PC (10 to 13%) correlated well with the increase of C16 (8 to 11%) fatty acyl chains on the *sn-1* position in *AAPT* RNAi plants (Figures 9A and 9B), indicating that the major contribution of the C34 PC increase in *AAPT* RNAi plants comes from the eukaryotic pathway, while ~2% of PC in *AAPT* RNAi plants can be attributed to prokaryotic lipids. In addition, the level of 16:0 fatty acids increased (Figure 9C), while no significant amounts of signature prokaryotic fatty acids (16:1 and 16:3) were detected in PC from both wild type and *AAPT* RNAi plants, and no overall increase of these signature prokaryotic fatty acids can be observed in the total lipids from *AAPT* RNAi plants compared with the wild type (Supplemental Figure 10). These results suggest that the remodeling of phospholipid composition and maintained PC level in *AAPT* RNAi plants is not likely the result of the export of prokaryotic lipids.

The maintained PC level in all the *aapt1/2* single and hemizygous mutant plants as well as all the strong *AAPT* RNAi plants is unexpected and may be compensated for by other lipid biosynthesis genes and pathways. One possibility is that the expression levels of lipid metabolism enzymes are altered by the knockdown of *AAPTs*. To test this, qPCR was performed to identify changes in the expression level of genes in the Kennedy pathway and the methylation process of P-Eth/PE in both leaves and seeds of R56, R104, and R125 lines. We examined the expression level of genes encoding choline kinase, ethanolamine kinase, choline-phosphate cytidylyltransferase, ethanolamine-phosphate

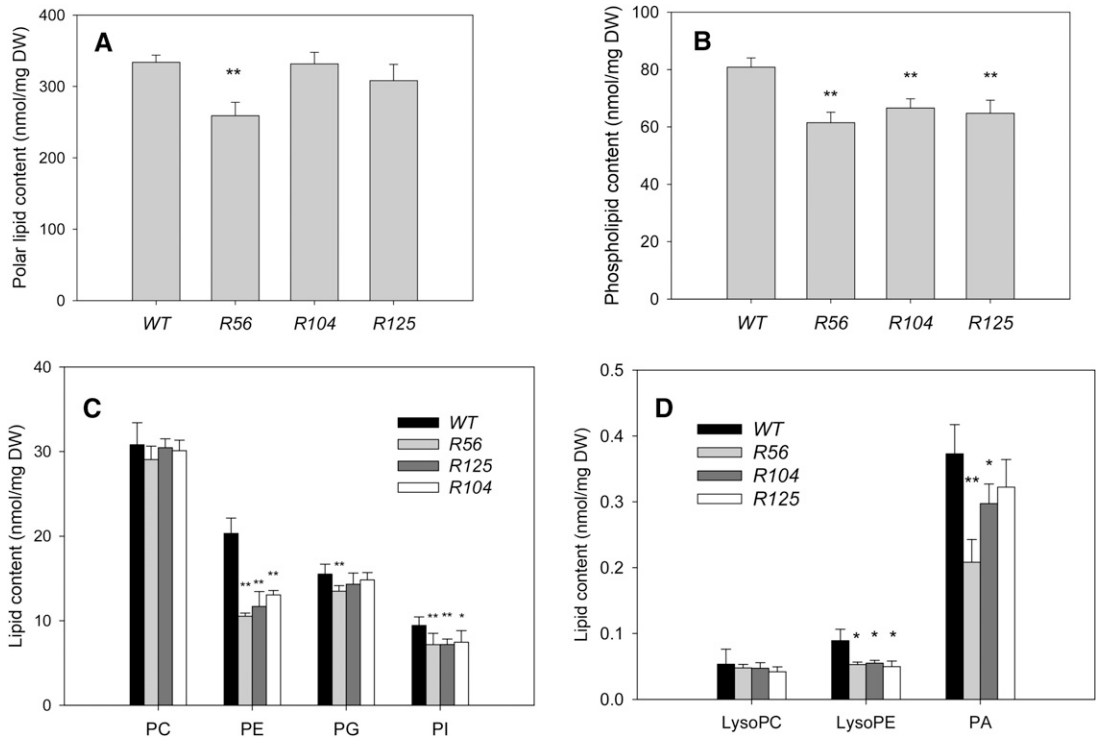

Figure 7. Leaf Polar Lipid Content of *AAPT* RNAi (R56, R104, and R125) Plants.

Lipids from the leaves of *AAPT* RNAi and wild-type plants were analyzed. Single and double asterisks mark differences between the wild type and the mutant at $P < 0.05$ and $P < 0.01$, respectively, based on Student's *t* test. Values are means ± SD ($n \geq 4$).

(A) Total content of phospholipids and galactolipids.

(B) Phospholipid content.

(C) Content of PC, P-Eth, PI, and PG.

(D) Content of LysoPC, LysoPE, and PA.

cytidylyltransferase, phospholipid *N*-methyltransferase, and PEAMT. A significant change of transcript abundance was not observed in any of these genes in either leaf or seed tissues, except that ethanolamine-phosphate cytidylyltransferase transcripts in seeds of the three strong *AAPT* RNAi lines had a moderate 1-fold increase (Supplemental Table 3). We also did not observe any significant change in the expression level of genes that encode enzymes in the CDP-DAG pathway.

AAPTs Affect PC and PE Production Differently

To determine the effect of AAPTs on PE and PE production in plants, we labeled seedlings with [^{3}H]-ethanolamine or [^{3}H]-choline to follow the head group incorporation into PC and PE in wild-type and *AAPT*-altered plants. Compared with the wild type, *AAPT* KO and RNAi plants were decreased in [^{3}H]-PC production, with wild type > *aapt2-1* > *aapt1-1* > *AAPT* RNAi for the labeling rate of [^{3}H]-PC (Figure 10A). The different rate of [^{3}H]-PC production is consistent with that of total lipid analysis, indicating that *AAPT1* contributes more than *AAPT2* to PC production in vegetative tissues. With [^{3}H]-ethanolamine labeling, [^{3}H]-PE increased continuously in the wild type (Figure 11A). However, *AAPT* KO and RNAi lines displayed a very different pattern of [^{3}H]-PE formation from the wild type. *AAPT* KO and RNAi lines had higher PE labeling rates than the wild type in the first 6 min (Figure 11B), but the increase plateaued within 30 min in *aapt1-1* and *aapt2-1* and for *AAPT* RNAi seedlings no further increase occurred after the first 6 min (Figure 11A).

One explanation for the tempered increase in [^{3}H]-PE in AAPT-deficient seedlings could result from an increase in conversion of [^{3}H]-ethanolamine or its derivatives into choline. To test this, we measured [^{3}H]-PC from the [^{3}H]-ethanolamine-fed seedlings. A small increase in [^{3}H]-PC was detected in all genotypes, but the formation of [^{3}H]-PC is much lower than that of [^{3}H]-PE (Figure 11C). In addition, we pulse-chased the [^{3}H]-ethanolamine-labeled seedlings to test if the labeled PE is converted to PC. While no decrease of [^{3}H]-PE could be seen in wild-type and *aapt1/2* KO lines, [^{3}H]-PE decreased in *AAPT* RNAi plants after 1 h of chase period. On the other hand, [^{3}H]-PC decreased rather than increased after the chase period in the wild type and all mutant lines (Figure 11D), suggesting no conversion from [^{3}H]-PE to [^{3}H]-PC occurred during the chase period. This result indicates that methylation of ethanolamine is not a major contributor to PC formation and this process is not altered by AAPT mutations.

The increase in C34 PC species and decrease in C34 species of PE and PI could result from the head group exchange between PC

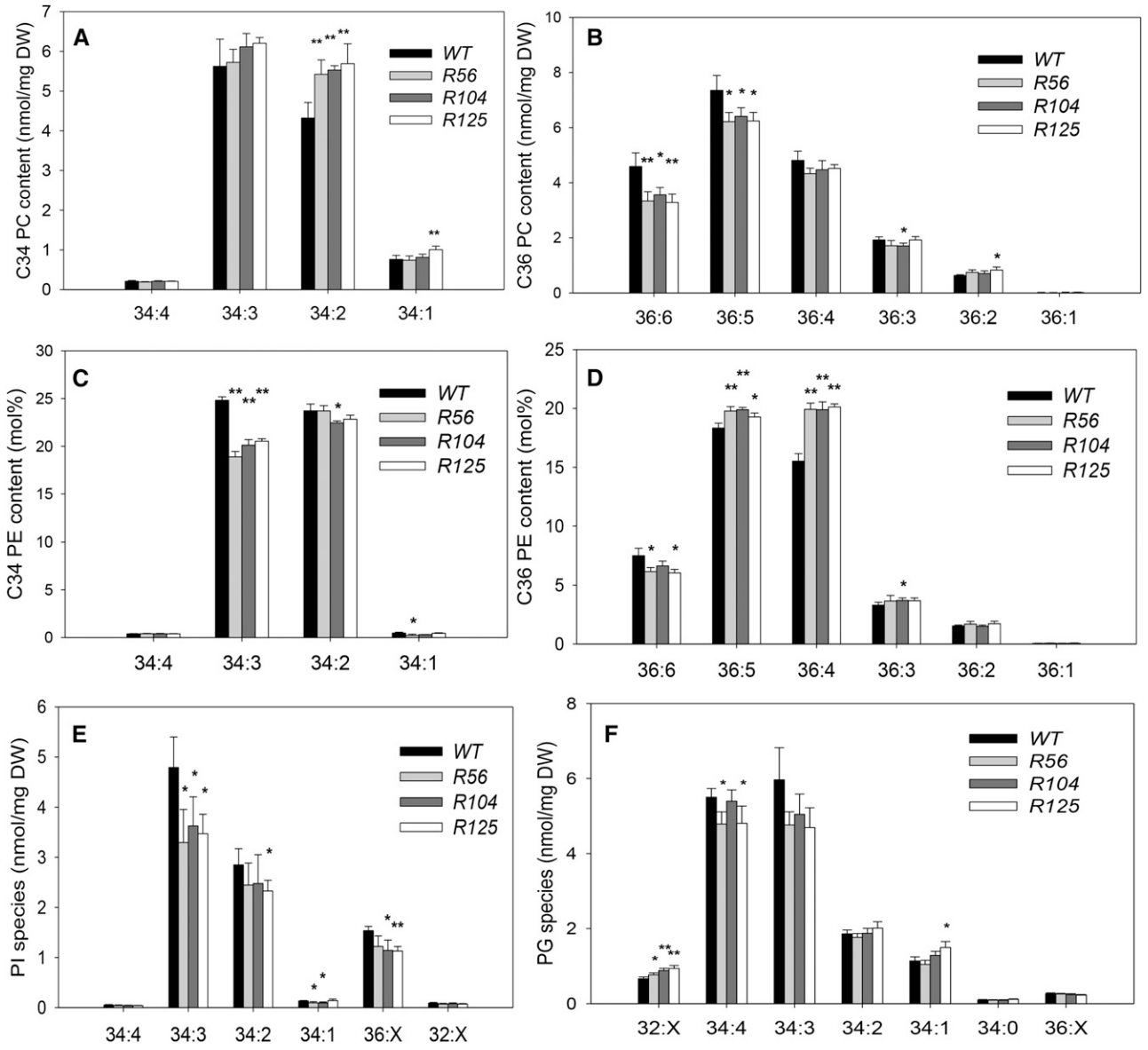

Figure 8. Changes in PC, PE, PI, and PG Species in *AAPT* RNAi (R56, R104, and R125) Plants.

Lipids from leaves of three *AAPT* RNAi lines were compared with the wild type. Single and double asterisks mark differences between the wild type and mutant at $P < 0.05$ and $P < 0.01$, respectively, based on Student's *t* test. Values are means ± SD ($n \geq 4$).

(A) Increases in PC C34 species.
(B) Decreases in PC C36 species.
(C) Decreases in PE C34 species.
(D) Increases in PE C36 species.
(E) Decreases in PI C34 species.
(F) Decrease in PG C34 species.

and PE/PI and/or methylation of PE to PC to maintain the PC level. To probe whether a head group exchange exists between PI and PC, we coinfiltrated C34:1 PI and choline into wild-type and *AAPT* RNAi leaves. The results showed the successful infiltration of PI 34:1 (Supplemental Figure 11A) but no corresponding increase of PC 34:1 (Supplemental Figure 11C) in either wild-type or *AAPT* RNAi leaves. However, we observed decreased levels of C34:3 PI (Supplemental Figure 11A) and increased lysophosphatidylcholine (lysoPC) species (Supplemental Figure 11B) in *AAPT* RNAi samples after infiltration, suggesting the existence of an indirect conversion route between PI and PC, which may be elevated in *AAPT* RNAi plants. In addition, the content of free choline in AAPT RNAi plants was comparable to that of the wild type (Supplemental Figure 12).

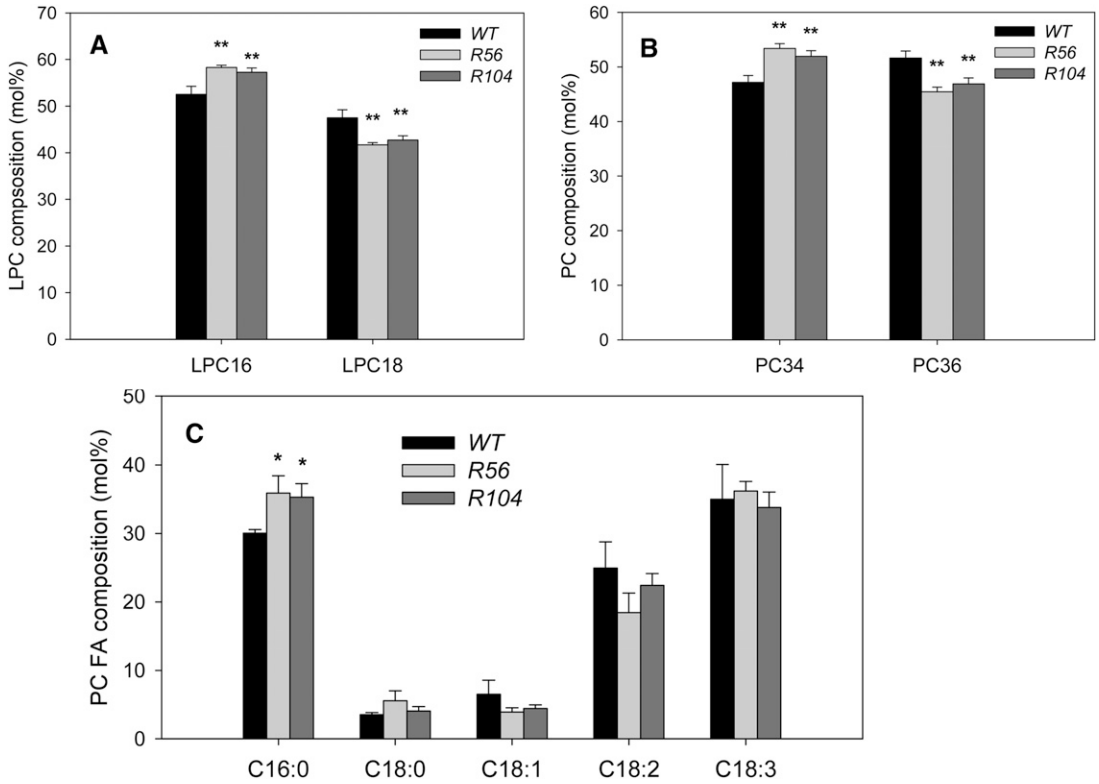

Figure 9. Fatty Acid Position Analysis and Fatty Acid Composition in PC and Total Lipids in *AAPT* RNAi (R56, R104, and R125) Plants.

Total lipids were digested by PLA_2, followed by analysis of PC and lysoPC by mass spectrometry. Single and double asterisks mark differences between the wild type and mutant at $P < 0.05$ and at $P < 0.01$, respectively, based on Student's *t* test. Values are means ± SD ($n = 3$).
(A) Content of lysoPC with C16 and C18 fatty acids after PLA_2 treatments of lipids from two *AAPT* RNAi lines and wild-type plants.
(B) Content of PC with C34 and C36 fatty acids without PLA_2 treatments of lipids from two *AAPT* RNAi lines and wild-type plants.
(C) Fatty acid composition of PC isolated from leaves of two *AAPT* RNAi lines and wild-type plants.

DISCUSSION

This study of AAPTs, which catalyze the last step of the Kennedy pathway for PC and PE biosynthesis, has led to several unexpected findings. In particular, deficiency in *AAPT1* and *2* does not result in a decrease in the total content of PC, but the molecular species of PC shifted significantly, with an increase in C34 PC and a decrease in C36. An opposite shift of molecular species occurred in PE/PI/PG, and the content of these phospholipids, particularly PE, is decreased in *AAPT*-deficient plants. The results suggest that a complicated compensatory network exists among different lipid metabolic pathways. However, this compensation has limitations, beyond which severe growth and reproductive defects become evident.

AAPT1 and *2* Are Essential for Pollen and Seed Development

The failure to obtain *aapt1/2* double KO homozygotes suggests the *AAPTs* are essential for plant reproduction and growth. Pollen is known to be susceptible to both environmental stress and gene defects, which may result from its haploid genome and lack of organelles. Arabidopsis pollen contains plastids in its vegetative cells, but the function of these plastids is to store starch rather than photosynthesis (Fujiwara et al., 2010). The sperm cells in Arabidopsis pollen are completely devoid of organelles, which coincide with the highly upregulated *AAPT1* and *AAPT2* transcript level. It is possible that the lack of the prokaryotic lipid-producing pathway that occurs in chloroplasts makes pollen highly dependent on lipids produced from the eukaryotic pathway. A similar scenario may also occur in developing seeds, in which much fewer active chloroplasts exist compared with leaf tissue. In addition, maturing seeds actively undergo oil accumulation by producing triacylglycerol, which not only requires DAG from an early step of the Kennedy pathway but is also proposed to acquire unsaturated fatty acids from membrane lipids, especially PC. Therefore, the blockage of the last step of the Kennedy pathway in the absence of a complementary lipid production pathway may disrupt normal embryo development and/or oil accumulation, leading to the aborted or severely wrinkled seeds we observed in the siliques of *aapt1/2* hemizygous plants.

We observed an aberrant segregation ratio in the progenies of both single homozygous hemizygotes, i.e., 1:5 and 1:18 (hemizygote: single KO). Compared with the predicted ratio of 1:1 due to the death

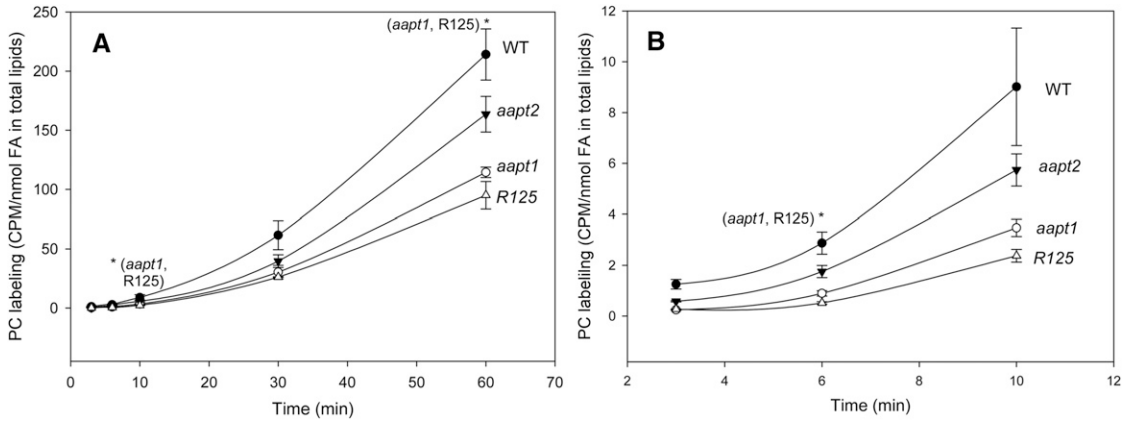

Figure 10. [^{3}H]-Choline Incorporation into PC in Wild-Type and AAPT Mutant (*aapt1*, *aapt2*, and R125) Seedlings.

Wild-type and mutant seedlings (10 d old) were incubated with media containing [^{3}H]-choline for 3, 6, 10, 30, and 60 min. Total lipids were extracted and separated on TLC. PC was collected and [^{3}H]-PC was determined and expressed as cpm/nmol fatty acids of total lipids. Values are means ± SE (n = 3). Asterisks mark differences between the wild type and mutants at $P < 0.05$ based on Student's t test.

(A) Time course of [^{3}H]-PC labeling over 60 min.

(B) Time course of [^{3}H]-PC labeling over the first 10 min.

of *aapt1/aapt2* double KO pollen, these segregation results suggest that 40% of embryos/seeds from *aapt1/AAPT1 aapt2/aapt2* and 47% of embryos/seeds from *aapt1/aapt1 AAPT2/aapt2* are not able to survive to the next generation. However, we did not observe as many aborted/wrinkled seeds in the siliques of *aapt1/2* hemizygous plants. This discrepancy may result from selection pressure during megasporogenesis, when only one out of four megaspores survives and develops into embryo sacs after the meiosis of the megasporocyte (Yadegari and Drews, 2004). These haploid megaspores in *aapt1/2* hemizygous plants will have two different genotypes: *aapt1/aapt2* and *aapt1/AAPT2* (or *AAPT1/aapt2*). According to what was discussed above, *AAPT* genes may be more indispensable in nonphotosynthetic tissue, and we expect a strong selection pressure against the *aapt1/2* double KO megaspores; thus, many more single KO megaspores may develop into embryo sacs before pollination.

AAPT1 and *AAPT2* Are Required for Normal Plant Growth

The lack of an aberrant growth phenotype in *aapt1/2* KO/hemizygotes and the inability to generate *aapt1/2* double KO homozygotes make it challenging to pinpoint the role of *AAPT1* and *AAPT2* in the vegetative growth of plants. Thus, we employed AAPT RNAi to knock down the transcript level of both *AAPT* genes in Arabidopsis. The highly conserved sequence between *AAPT1* and *AAPT2* makes it possible to knockdown both genes with a single construct. We introduced the construct into the wild-type, *aapt1 KO*, and *aapt2 KO* background, in order to ensure high knockdown efficiency. Repeated screening of seeds from transformed plants identified most transgenic plants carrying the RNAi DNA from the *aapt1* KO background but no positive lines from the *aapt2* KO background. All *AAPT* RNAi plants under the *aapt1* background did not show significant alterations in growth, and the lack of phenotype might result from ineffective RNAi suppression because the *AAPT* RNAi construct was made using the *AAPT1* sequence, while *AAPT2* is not a preferred target (Supplemental Table 1). On the other hand, it is not surprising that no positive *AAPT* RNAi plants in the *aapt2* KO background were recovered because *AAPT1* is the preferred target of the RNAi construct and plants lacking both *AAPT2* and *AAPT1* functions would not survive. We did observe many nongerminating seeds on plates when screening transgenic T1 *AAPT* RNAi seeds in the *aapt2* background.

During screening, we identified a number of positive RNAi transgenic seeds in the wild-type background (as the RNAi construct carries dsRed and the positive seeds are red), but most seeds either did not germinate or the seedlings died early on the plate. The three RNAi lines in the wild-type background exhibited retarded growth. The finding that the RNAi phenotype was more severe in the wild-type background than in the *aapt1* KO background may be explained by the secondary small interfering RNA (siRNA) production after the degradation of the original target mRNA (Baulcombe, 2007). Since *AAPT2* is not the preferred target of the dsRNA construct, the primary siRNAs produced by the construct may not be able to degrade *AAPT2* mRNA effectively in the absence of *AAPT1* transcripts in the *aapt1* KO background, while in the wild-type background, the degradation of *AAPT1* transcripts by the primary siRNAs may trigger amplified secondary siRNA production that may in turn degrade *AAPT2* transcripts at a higher efficiency. Furthermore, the cauliflower mosaic virus 35S promoter used in the dsRNA construct is inactive in pollen (Wilkinson et al., 1997), so no segregation problem was observed in any of these *AAPT* RNAi plants, although it is not known how effective the 35S promoter is in megaspores.

As PC and PE are important eukaryotic membrane lipids, a large decrease in *AAPT* transcript level led to plant growth arrest. The phenotype severity is positively associated with the degree of decrease in *AAPT* transcript in *AAPT* RNAi plants, further supporting the essential role of *AAPT1* and *AAPT2* in normal plant growth. However, no major difference was observed in the lipid composition among the three strong RNAi lines under the wild-type background. Even between R56 heterozygous

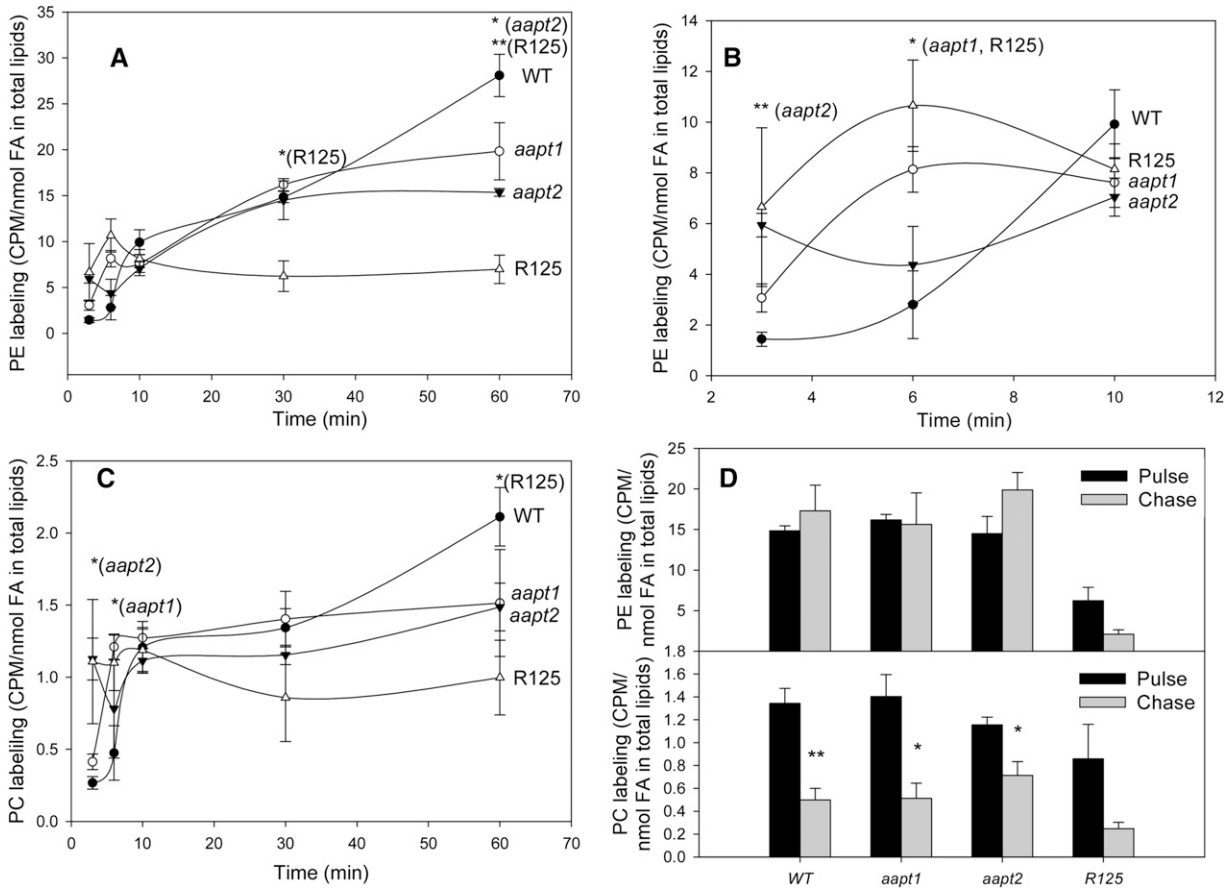

Figure 11. [^{3}H]-Ethanolamine Incorporation into PE and PC.

Wild-type and *AAPT* mutant (*aapt1*, *aapt2*, and R125) seedlings (10 d old) were incubated with media containing [^{3}H]-ethanolamine for 3, 6, 10, 30, and 60 min. Total lipids were extracted and separated on TLC. PE and PC were collected, and [^{3}H]-PE and [^{3}H]-PC were determined and expressed as cpm/nmol fatty acid in total lipids. Values are means ± SE ($n = 3$). Single and double asterisks mark differences between the wild type and mutants at $P < 0.05$ and $P < 0.01$, respectively, based on Student's *t* test.

(A) [^{3}H]-PE produced over 60 min.

(B) [^{3}H]-PE produced over the first 10 min.

(C) [^{3}H]-PC produced over 60 min.

(D) Pulse-chase labeling of [^{3}H]-PE and [^{3}H]-PC. Seedlings were incubated with [^{3}H]-ethanolamine for 30 min and then transferred to labeling free media for 60 min, followed by lipid extraction and analysis. Values are means ± SE ($n = 3$). Single and double asterisks mark differences before and after chase at $P < 0.05$ and $P < 0.01$, respectively, based on Student's *t* test.

and homozygous plants, although their phenotype severities and knockdown levels of *AAPT* genes are quite different, no further changes in lipid composition occurred between homozygous and heterozygous plants. This may suggest that such lipid changes (~40% decrease of PE and C36-C34 species shift in PC) have reached a threshold that plants require to survive. Further decreases in the *AAPT* transcript level may only slow down the accumulation of essential lipids and thus retard the vegetative growth rate rather than further change the lipid composition.

Maintaining a Homeostatic Level of PC Is Essential for Plant Growth and Development

The high similarity in sequence and catalytic activity between Arabidopsis AAPT1 and AAPT2 suggests that these proteins share overlapping functions, which is also supported by the lack of growth phenotype in the *aapt1/2* KO and hemizygotes. However, our lipid profiling data suggest that *AAPT1* plays a more important role than does *AAPT2* in vegetative tissues, since *aapt1* KO-related mutants showed more lipid changes than *aapt2* KO-related mutants in terms of number of different classes of lipids changed and the amount decreased, in agreement with the fact that *AAPT1* is expressed at much higher levels than *AAPT2* in rosette leaves. The direct phospholipid products of the Kennedy pathway are PC and PE (Figure 12). In addition, it was reported that the yeast-produced AAPT1 and AAPT2 enzymes show different substrate preferences in vitro. Although both enzymes are more efficient in producing PC, AAPT2 has an even higher preference for PC production than AAPT1 (Goode and Dewey, 1999). The decrease of PE in *aapt1* KO related mutants

(*aapt1-1* and *aapt1/2* hemizygotes) is most likely related to the higher expression level of *AAPT1* in rosette leaves, and it might be possible that AAPT1 in planta has more EPT activity for PE synthesis, thus resulting in the decrease in PE level in the AAPT-deficient plants. Our radiolabeling data support the former hypothesis. The higher labeling rate of PC than PE may play an important role in the unexpected lipid species change observed. In addition, the *aapt1-1* and *aapt2-1* seed lipid data showed similar change in species, which is also consistent with the expression profile of *AAPT1* and *AAPT2* in different tissues.

In addition to AAPTs, PE may be produced by the decarboxylation of PS (Figure 12). A previous report suggests that PS in plants was not a significant source of PE production. For instance, a triple mutant of Arabidopsis PS decarboxylases only had a mild decrease of PE in mitochondria (Nerlich et al., 2007). On the other hand, we observed an increase in PE species with long-chain fatty acids in *AAPT* KO/RNAi lines, and PS contains a higher percentage of long-chain FAs than other species. In addition, one PS synthase (PSS1) was found in the Arabidopsis genome, which is of base-exchange type and uses PE and serine as substrates (Yamaoka et al., 2011). The small increase of PE with long-chained fatty acids could mean that some PS is converted to PE via the CDP-DAG pathway and/or the base-exchange pathway (Figure 12).

Our study shows that despite the large decrease in PE, the PC level is comparable between wild-type and AAPT-deficient plants. Some previous studies on enzymes in the Kennedy pathway showed different levels of lipid composition changes. Noticeably, gene knockout of CTP:phosphorylcholine cytidylyltransferases 1 or 2, which catalyze the step before AAPT reactions in the Kennedy pathway, resulted in no significant changes of PC levels in Arabidopsis (Inatsugi et al., 2009), while a partial loss of function of CTP:phosphorylethanolamine cytidylyltransferase showed a relative decrease in PE and increase in PC levels (Mizoi et al., 2006). In addition, in the *xipotl1* (*peamt1*) mutant, PC level was decreased by 22% in roots and 18% in leaves, leading to aberrant root development and root epidermal cell integrity, while rosettes of this mutant had no overt phenotypic changes (Cruz-Ramírez et al., 2004). In mammalian cells, disruption of PC production led to cell death (Cui et al., 1996). Together, these results suggest that maintaining a certain level of PC is essential for normal eukaryotic functions, while in green tissue, additional pathways for lipid production may help alleviate mild decreases in PC content.

The change of membrane lipid composition may have other consequences. This may be attributed to the change of membrane structure and fluidity since PC and PE are different in head group size and shape. PC favors the formation of lipid bilayers because of its cylindrical shape and is present in a high level in the outer leaflet of the plasma membrane. In contrast, PE is present mostly in the inner leaflet of the plasma membrane because of its cone shape and small head group. PE on its own forms inverted hexagonal phases. When present with other lipids in a bilayer, PE gives a lateral pressure that modulates membrane curvature and stabilizes membrane proteins and plays a role in membrane fusion (van den Brink-van der Laan et al., 2004). A study on *AAPT1* in wheat (*Triticum aestivum*) indicates that the PC/PE ratio plays a role in cold acclimation (Sutoh et al., 2010). *AAPT* mutants have increased PC/PE ratios as well as changed acyl-chain composition in PC. It will of interest in the future study to explore how these

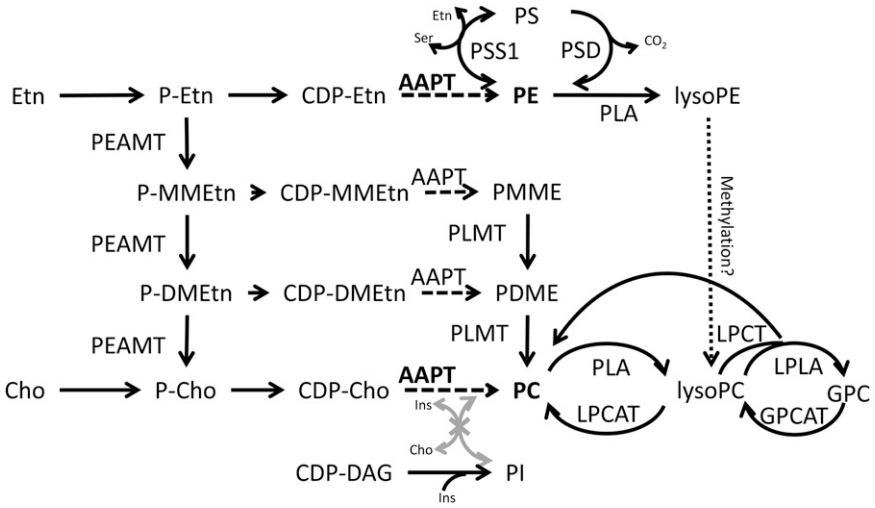

Figure 12. Possible Mechanisms of PC Compensation in *AAPT*-Deficient Plants.

AAPTs are primarily responsible for the de novo PC and PE production in plants. PS may contribute to PE production by head group exchange and/or decarboxylation, while lysoPE may be methylated to form lysoPC, which may contribute to PC formation via acyltransferases such as GPCAT and LPCAT. Etn, ethanolamine; Cho, choline; MMEtn, monomethylethanolamine; DMEtn, dimethylethanolamine; Ins, inositol; GPC, glycerophosphocholine; CDP-DAG, cytidine diphosphate diacylglycerol; PMME, phosphatidylmonomethylethanolamine; PDME, phosphatidyldimethylethanolamine; PLMT, phospholipid methyltransferase; PSS1, PS synthase 1; PSD, PS decarboxylase; PL, phospholipase A; LPCAT, LPC acyltransferase; LPCT, LPLA lysophospholipase A; LPCT, LPC transacylase leading the formation of GPC and PC from two lysoPCs. Dashed lines denote activity compromised, and dotted line indicates hypothetical activity based on the data.

lipids changes impact plant performance under challenging conditions.

How Is the PC Level Maintained?

AAPT1 and AAPT2 catalyze the last step in the Kennedy pathway, which are required for PC and PE synthesis, as well as the plant-specific methylation pathway, so we expected a concurrent decrease in PC and PE levels in *AAPT1*- and *AAPT2*-deficient plants (Figure 12). Thus, the finding that PC level remains unchanged in the *aapt1/2* KO, *aapt1/2* hemizygotes, and *AAPT* RNAi mutant plants is highly unexpected. How is the PC level maintained in *AAPT*-deficient plants? What pathways/enzymes are involved in the compensation of PC level?

Our transcriptional profiling results indicate that the change of the gene expression in the eukaryotic pathway for glycerolipid production is not responsible for the lipid composition changes in *AAPT* RNAi plants with a well maintained PC level. Based on the lipid profiling data, several possible hypotheses can be proposed to explain this preservation of PC homeostasis. First, PE may be converted to PC directly or indirectly (Figure 12). The lack of PE methyltransferase activity in most plants including Arabidopsis suggests the conversion may go through a more complicated route. Our [^{3}H]-ethanolamine labeling and pulse-chase assay suggest the direct conversion of PE to PC is not a significant source of PC production. Our data showed decreased lysoPE in all the *aapt1/2* KO, *aapt1/2* hemizygotes, and *AAPT* RNAi lines. The turnover rate of PE is likely decreased in these mutant plants. It is possible that some of the lysoPE is converted to its methylated form by a currently unknown mechanism and then reacylated to produce PC as the final product (Figure 12). In addition, the recently reported enzyme glycerophosphocholine acyltransferase (GPCAT), which acylates glycerol-3-phopshocholine to synthesize lysoPC (Stålberg et al., 2008; Lager et al., 2015), may contribute to the reproduction of lysoPC in AAPT-deficient plants. Glycerol-3-phopshocholine is believed to be produced from deacylation of PC, rather than through de novo PC biosynthesis. However, GPCAT may help maintain PC level by recycling glycerol-3-phopshocholine GPC in *AAPT*-deficient plants (Figure 12).

PEAMT, known to convert P-Eth to phosphocholine, may play a role in the shift of production from PE to PC by altering the substrate availability, despite its lack of transcript level change in *AAPT*-deficient lines, since PEAMT was reported to be post-transcriptionally regulated by its upstream open reading frame (Tabuchi et al., 2006), and its activity was also reported to be inhibited by PA in wheat (Jost et al., 2009). Particularly, the decreased level of PA in *AAPT* RNAi lines may derepress the activity of PEAMT and promote PC production in these plants.

The acyl composition of PC differs greatly from the wild type in AAPT-suppressed plants. The increase in C34 PC occurs with a concomitant decrease in C36 PC, while PE showed an opposite change with a decrease in C34 and increase in C36 species. The increased level of C34 PC species might indicate that prokaryotic lipids play a role in the compensation of PC level in AAPT-deficient plants. However, our fatty acyl chain position analysis does not support the existence of a significant amount of prokaryotic lipids in PC, either in the wild type or in *AAPT* RNAi lines. In contrast, the increase of C34 PC species is very well explained by the increase of C16 fatty acid in the *sn-1* position of PC in *AAPT* RNAi plants. The contribution of prokaryotic lipids is likely very small (~2%) in the compensation of PC. We also did not observe overall increased prokaryotic lipid production in response to blockage of the Kennedy pathway. The PE species that was most decreased was 34:3 PE, whereas 34:2 PC exhibited the greatest increase. The different PC and PE species argue against a direct conversion for C34 PE to C34 PC. One plausible explanation is the differential substrate preference of AAPTs in plants: AAPTs prefer C36 PC and C34 PE, thereby resulting in a decrease in both C36 PC and C34 PE in AAPT-deficient plants.

In addition to PE, we also observed decreased PI and PG levels in the leaf samples of *AAPT* RNAi lines. PI and PG are produced via the CDP-DAG pathway rather than the Kennedy pathway. The biosynthesis of PI happens predominantly in the ER, while PG can be synthesized in the ER and plastids. The species of PI that declined the most are 34:3 PI and 34:2 PI, while the largest decrease was observed in 34:4 PG and 34:3 PG species. In comparison, PC is increased in 34:3 and 34:2 species. This species difference argues against a direct conversion of PI to PC by head group exchange. Consistent with this, we did not observe a significant increase of 34:1 PC when 34:1 PI and choline were coinfiltrated into the leaves of wild-type or *AAPT* RNAi lines. On the other hand, PI and PG can be degraded to provide precursors for PC production, which would still need the activity of AAPT (Figure 12).

Collectively, our data indicate that the reaction catalyzed by AAPT1 and 2 in the Kennedy pathway is the major pathway for PC synthesis in Arabidopsis leaves and seeds. AAPT1 and AAPT2 have overlapping functions, but AAPT1 contributes more than AAPT2 to PC production in vegetative tissues (Figure 12). There is no head group exchange between PI and PC, and the methylation of ethanolamine or PE contributes little to PC production even in AAPT-deficient plants. Considering the embryonic lethality of the *aapt1/2* double KO and the retarded growth phenotype of the *AAPT* RNAi lines, AAPTs are indispensable for PC production and plant growth and reproduction.

METHODS

Plant Materials and Growth Conditions

Arabidopsis thaliana wild-type (Columbia-0) and T-DNA insertion lines of *aapt1* (SALK_059178) and *aapt2* (SALK_150255) were obtained from the ABRC (Ohio State University). The homozygous KO mutants were isolated by PCR screening using pairs of gene-specific primers for *AAPT1* (5′-GAGTGATCAACTAAGAGTCTTTTC-3′ and 5′-GTTTTGCATCAATACAACATTG-3′) and *AAPT2* (5′-TGTATTTTACACTGAAAAATGGG-3′ and 5′-CGACAATGCACCAACTATGTC-3′), with a T-DNA left border primer (LBa1, 5′-TGGTTCACGTAGTGGGCCATCG-3′). Complementation lines were generated by cloning the whole genome sequences (including the promoter region and terminator region) of *AAPT1* (by 5′-TTTGGCGCGCCTTCTTCGTTTGGTCACTCACTC-3′ and 5′-TTTGGCGCGCCTTATTGCCCATTTTGTAGGTTC-3′) and *AAPT2* (by 5′-TTTGGCGCGCCATGTCTTCTCGATTCCTCCT-3′ and 5′-TTTGGCGCGCCGTGTTGTTTTGTTCCGTTGT-3′) to the *Asc*I cloning site of binary vector pEC291, followed by transformation of wild-type plants by floral dipping. *AAPT* RNAi lines were generated by cloning

the 500-bp (1 to 500 bp) open reading frame of *AAPT1* in sense (by 5′-AAGCGCTCGAGATGGGTTACATAGGAGCTCATG-3′ and 5′-AAGCGGGTACCAGAATAAGTGTGTTGGTGAAATAGT-3′) and antisense (by 5′-AAGCGTCTAGAATGGGTTACATAGGAGCTCATG-3′ and 5′-AAGCGAAGCTTAGAATAAGTGTGTTGGTGAAATAGT-3′) directions to the RNAi vector pKannibal (into the *Xho*I and *Kpn*I sites for the sense fragment, and *Xba*I and *Hin*dIII sites for the antisense fragment), and then the sense-antisense dsRNA *AAPT* cassette was cloned into the expression vector pBin35SRed1 by enzyme digestion, blunt end treatment, and ligation, followed by wild-type plant transformation. For screening, Arabidopsis seeds were surface-sterilized by 70% (v/v) ethanol and 50% (v/v) bleach solution, followed by sterilized water wash (three to six times). The sterilized seeds were then spread and germinated on a 0.5× Murashige and Skoog (MS) plate with proper antibiotics. For transplanting, 1- to 2-week-old seedlings (or until true leaves appeared) from plates were transferred to soil in 5-inch pots, with up to four plants per pot. Plants were grown under 16-h 22°C light/8-h 18°C dark period in a plant growth chamber.

Transcript Analysis

RNA extraction and real-time PCR analysis of transcript levels were performed as described previously (Li et al., 2011). Total RNA was extracted from leaves or seeds using an RNeasy Mini Kit (Qiagen) or an adapted cetyltrimethylammonium bromide (CTAB) method, respectively. For the CTAB RNA extraction method, plant tissues were ground into fine power in liquid nitrogen and extracted by 2% CTAB solution. After phenol extraction, RNA was precipitated by 2 M LiCl. Before reverse transcription, DNA contamination was removed by Turbo DNase (Ambion). cDNA was synthesized using a qScript cDNA synthesis kit (Quanta Bioscience).

Real-time PCR was performed on a MyiQ real-time PCR detection system (Bio-Rad). SYBR green dye was used to detect the synthesis of PCR product. *Ubiquitin10* (*UBQ10*) was used as internal standard and for cDNA input adjustment (Ct $\approx$ 20 for *UBQ10*). PCR conditions were as follows: 95°C 3 min for 1 cycle; 95°C for 30 s, 60°C for 30 s, and 72°C for 30s for 40 cycles; final extension is 72°C for 10 min, followed by melting curve analysis. All primers used in real-time PCR are listed in Supplemental Table 2.

Double Mutant Generation and Segregation Analysis

To generate the *aapt1 aapt2* double mutant, homozygotes of *aapt1* KO and *aapt2* KO were crossed by removing the unopened anthers from the female parent flower and pollinated by the male parent flower. The F1 progenies were self-pollinated and F2 generation was screened by PCR using both *AAPT1* and *AAPT2* gene-specific primers and LBa1as described above. The segregation ratios of *aapt1/2* hemizygotes were obtained by growing the self-pollinated seeds from previously identified *aapt1/2* hemizygotes and screening by PCR. More than three rounds of screening results were pooled. χ^2 analysis was used to test the difference between the actual segregation and theoretical ratios.

Pollen Viability Analysis and Seed Development

A viability staining method using FDA/PI was used for pollen viability analysis (McConn and Browse, 1996). FDA was diluted to 5 μg/mL final concentration, and PI was used at 2 μg/mL final concentration in 15% sucrose solution just prior to the experiment. One drop of the FDA/PI staining solution was spotted on glass slides, and detached anthers were stirred in the solution to obtain a sufficient number of pollen grains. A cover glass was then applied and the stained pollen was observed under confocal microscopy (Zeiss LSM 700). Viable pollen is stained green by fluorescein that is produced by active esterases, while dead pollen is stained red due to increased membrane permeability to PI. For the seed development assay, maturing siliques (10 to 14 d after pollination) were used. Siliques were dissected and observed under a stereomicroscope.

Lipid Extraction and Analysis

Polar lipids were extracted and analyzed by a liquid chromatography-mass spectrometry (LC-MS)-based method as described before (Welti et al., 2002). Briefly, fresh tissues (leaves or seeds) were immersed in hot (75°C) isopropanol for 15 min to inactivate PLD activity. Then, five more extractions using chloroform/methanol (2:1 v/v, with 0.01% butylated hydroxytoluene) were performed and the six extracts were combined. After extractions by 1 M KCl and water, lipid phases were dried under nitrogen gas. The resulting lipids were diluted and applied to the LC-MS (API 4000) detection system, and data were processed by Analyst 1.5.1.

PLA_2 Treatment and Leaf Fatty Acid Position/Composition Analysis

Total leaf lipids were dried and dispersed in 500 μL reaction buffer (100 mM HEPES, pH 7.4, 10 mM $CaCl_2$, and 10 mM $MgCl_2$) by sonication. Ten units of PLA_2 from honeybee venom (Sigma-Aldrich) were added to start the reaction at 37°C for 2 h. The reaction was terminated by the addition of 500 μL of 500 mM NaCl and 2 mL methanol/chloroform (2:1, v/v). The lower phase was transferred to a separate tube. Two additional extractions with 1 mL chloroform were performed, and the organic phases were combined and subjected to LC-MS-based lipid analysis. Untreated lipids were used as control.

For leaf fatty acid composition analysis, 10 μg total lipids was dried and analyzed by transmethylation and gas chromatography with a flame ionization detector. For PC fatty acid composition analysis, total leaf lipids were separated on TLC, and then the PC spot was recovered and analyzed by transmethylation and gas chromatography (Li et al., 2011).

Leaf Infiltration with PI and Choline

Young leaves were harvested and several wounds were cut to facilitate the infiltration. C34:1-PI (1 μg) was dried under N_2 gas and rehydrated with 100 μL 0.1% Silwet L-77 and 10 μg choline chloride, followed by sonication to disperse the lipids. Ten microliters of the solution was spotted on each leaf disc and infiltrated under vacuum for 1 h. Leaf discs treated with the same solution but without added PI, and choline was used as control. Lipid was extracted and profiled as described above.

Choline and Ethanolamine Labeling

Radioisotope labeling of seedlings was adapted from a method reported previously (Bates et al., 2012). Twenty seedlings were used for each sample and grown in media (0.5× MS media with 0.5% sucrose, pH 5.8) in 24-well cell culture plates under 24 h light at 22°C for 10 d. [^{3}H]-choline (choline chloride [methyl-3H]; American Radiolabeled Chemicals; ART-0197) or [^{3}H]-ethanolamine (ethanolamine [1-^{3}H] hydrochloride; American Radiolabeled Chemicals; ART-0216) were added to labeling medium (5 mM MES and 0.5× MS media with 0.5% sucrose, pH 5.8) at a final concentration of 0.5 μCi/mL. Labeling was initiated by transferring the seedlings to the [^{3}H]-choline- or [^{3}H]-ethanolamine-containing medium. At 3, 6, 10, 30, and 60 min, labeled seedlings were quickly transferred to a tube containing preheated (>75°C) isopropanol with 0.01% butylated hydroxytoluene to stop labeling and lipids were extracted as described previously. Three repeats were used for each line at each time point. For the pulse-chase assay, seedlings were incubated with the radiolabeled

substrate for 30 min and then transferred to labeling media without substrates for another 1 h before lipid extraction. An aliquot from each lipid extract was resolved on a TLC plate (chloroform:methanol:acetic acid:water = 85:15:12.5:3.5). PE and PC spots were collected and counted with a Tri-Carb liquid scintillation counter (Perkin-Elmer). The radioactivity of PC and PE was normalized to the total fatty acids in the sample, which was obtained by transmethylation of the aliquot from the same sample and quantified on gas chromatography with fatty acid 17:0 as internal standard (Li et al., 2011).

Accession Numbers

Sequence data from this article can be found in the GenBank/EMBL data libraries under the following accession numbers: *AAPT1*, *At1g13560*; *AAPT2*, *At3g25585*; and *UBQ10*, At4g05230.

Supplemental Data

Supplemental Figure 1. Secondary structure prediction of AAPT.

Supplemental Figure 2. Expression profile of AAPT1 and AAPT2 by Genevestigator.

Supplemental Figure 3. Total phospholipid content in wild-type, *aapt1/2* KO, and hemizygotes.

Supplemental Figure 4. C34 and C36 PE content in wild-type, *aapt1/2* KO, and hemizygotes.

Supplemental Figure 5. Major phospholipid species in wild-type and *aapt1/2* complementation plants.

Supplemental Figure 6. Root and root hair development in wild-type, *aapt1/2* KO, and *AAPT* RNAi lines.

Supplemental Figure 7. Segregation of *AAPT* RNAi (R56) heterozygotes.

Supplemental Figure 8. TLC and quantification of PC and PE from wild-type and *AAPT* RNAi (R56) plants.

Supplemental Figure 9. Phospholipid species in seeds of wild-type, *aapt1/2* KO, and *AAPT* RNAi plants.

Supplemental Figure 10. Leaf fatty acid composition of wild-type and *AAPT* RNAi plants.

Supplemental Figure 11. Lipid species change after PI-choline infiltration in wild-type and *AAPT* RNAi leaves.

Supplemental Figure 12. Free choline content in wild-type and *AAPT* RNAi plants.

Supplemental Table 1. Verification of targets of *AAPT* dsRNA construct.

Supplemental Table 2. Primers used for real-time PCR.

Supplemental Table 3. Transcriptional profiling of enzymes in the Kennedy pathway and methylation process in leaves and seeds of *AAPT* RNAi plants.

ACKNOWLEDGMENTS

We thank Ruth Welti and Mary Roth for generous gifts of lipid standards for lipid profiling. Work by Y.L. and X.W. was supported by the U.S. Department of Energy, Office of Science, Office of Basic Energy Sciences, Materials Sciences and Engineering Division under Award DE-SC0001295 and by National Science Foundation Grant IOS-0818740. Work by G.W. was supported by the by U.S. Department of Energy Grant DE-AR0000202.

AUTHOR CONTRIBUTIONS

X.W. designed the project. Y.L. and G.W. performed the experiments and analyzed the data. Y.L. and X.W. cowrote the article.

Received February 26, 2015; revised March 26, 2015; accepted April 14, 2015; published May 15, 2015.

REFERENCES

Bates, P.D., Fatihi, A., Snapp, A.R., Carlsson, A.S., Browse, J., and Lu, C. (2012). Acyl editing and headgroup exchange are the major mechanisms that direct polyunsaturated fatty acid flux into triacylglycerols. Plant Physiol. **160:** 1530–1539.

Baulcombe, D.C. (2007). Molecular biology. Amplified silencing. Science **315:** 199–200.

Bolognese, C.P., and McGraw, P. (2000). The isolation and characterization in yeast of a gene for *Arabidopsis* S-adenosylmethionine: phospho-ethanolamine N-methyltransferase. Plant Physiol. **124:** 1800–1813.

Browse, J., Warwick, N., Somerville, C.R., and Slack, C.R. (1986). Fluxes through the prokaryotic and eukaryotic pathways of lipid synthesis in the '16:3' plant *Arabidopsis thaliana*. Biochem. J. **235:** 25–31.

Carman, G.M., and Henry, S.A. (2007). Phosphatidic acid plays a central role in the transcriptional regulation of glycerophospholipid synthesis in *Saccharomyces cerevisiae.* J. Biol. Chem. **282:** 37293–37297.

Chapman, K.D., and Ohlrogge, J.B. (2012). Compartmentation of triacylglycerol accumulation in plants. J. Biol. Chem. **287:** 2288–2294.

Cruz-Ramírez, A., López-Bucio, J., Ramírez-Pimentel, G., Zurita-Silva, A., Sánchez-Calderon, L., Ramírez-Chávez, E., González-Ortega, E., and Herrera-Estrella, L. (2004). The *xipotl* mutant of *Arabidopsis* reveals a critical role for phospholipid metabolism in root system development and epidermal cell integrity. Plant Cell **16:** 2020–2034.

Cui, Z., Houweling, M., Chen, M.H., Record, M., Chap, H., Vance, D.E., and Tercé, F. (1996). A genetic defect in phosphatidylcholine biosynthesis triggers apoptosis in Chinese hamster ovary cells. J. Biol. Chem. **271:** 14668–14671.

Fujiwara, M.T., Hashimoto, H., Kazama, Y., Hirano, T., Yoshioka, Y., Aoki, S., Sato, N., Itoh, R.D., and Abe, T. (2010). Dynamic morphologies of pollen plastids visualised by vegetative-specific FtsZ1-GFP in *Arabidopsis thaliana.* Protoplasma **242:** 19–33.

Goode, J.H., and Dewey, R.E. (1999). Characterization of aminoalcoholphosphotransferases from *Arabidopsis thaliana* and soybean. Plant Physiol. Biochem. **37:** 445–457.

Inatsugi, R., Kawai, H., Yamaoka, Y., Yu, Y., Sekiguchi, A., Nakamura, M., and Nishida, I. (2009). Isozyme-specific modes of activation of CTP: phosphorylcholine cytidylyltransferase in *Arabidopsis thaliana* at low temperature. Plant Cell Physiol. **50:** 1727–1735.

Jost, R., Berkowitz, O., Shaw, J., and Masle, J. (2009). Biochemical characterization of two wheat phosphoethanolamine N-methyltransferase isoforms with different sensitivities to inhibition by phosphatidic acid. J. Biol. Chem. **284:** 31962–31971.

Keogh, M.R., Courtney, P.D., Kinney, A.J., and Dewey, R.E. (2009). Functional characterization of phospholipid N-methyltransferases from *Arabidopsis* and soybean. J. Biol. Chem. **284:** 15439–15447.

Lager, I., Glab, B., Eriksson, L., Chen, G., Banas, A., and Stymne, S. (2015). Novel reactions in acyl editing of phosphatidylcholine by lysophosphatidylcholine transacylase (LPCT) and acyl-CoA:glycerophosphocholine acyltransferase (GPCAT) activities in microsomal preparations of plant tissues. Planta **241:** 347–358.

Li, M., Bahn, S.C., Guo, L., Musgrave, W., Berg, H., Welti, R., and Wang, X. (2011). Patatin-related phospholipase pPLAIIIβ-induced changes in lipid metabolism alter cellulose content and cell elongation in *Arabidopsis.* Plant Cell **23:** 1107–1123.

McConn, M., and Browse, J. (1996). The critical requirement for linolenic acid is pollen development, not photosynthesis, in an Arabidopsis mutant. Plant Cell **8:** 403–416.

Mizoi, J., Nakamura, M., and Nishida, I. (2006). Defects in CTP: PHOSPHORYLETHANOLAMINE CYTIDYLYLTRANSFERASE affect embryonic and postembryonic development in *Arabidopsis.* Plant Cell **18:** 3370–3385.

Nerlich, A., von Orlow, M., Rontein, D., Hanson, A.D., and Dörmann, P. (2007). Deficiency in phosphatidylserine decarboxylase activity in the *psd1 psd2 psd3* triple mutant of *Arabidopsis* affects phosphatidylethanolamine accumulation in mitochondria. Plant Physiol. **144:** 904–914.

Noga, A.A., and Vance, D.E. (2003). Insights into the requirement of phosphatidylcholine synthesis for liver function in mice. J. Lipid Res. **44:** 1998–2005.

Ohashi, Y., Oka, A., Rodrigues-Pousada, R., Possenti, M., Ruberti, I., Morelli, G., and Aoyama, T. (2003). Modulation of phospholipid signaling by GLABRA2 in root-hair pattern formation. Science **300:** 1427–1430.

Ohlrogge, J., and Browse, J. (1995). Lipid biosynthesis. Plant Cell **7:** 957–970.

Sciara, G., et al. (2014). Structural basis for catalysis in a CDP-alcohol phosphotransferase. Nat. Commun. **5:** 4068.

Stålberg, K., Neal, A.C., Ronne, H., and Ståhl, U. (2008). Identification of a novel GPCAT activity and a new pathway for phosphatidylcholine biosynthesis in *S. cerevisiae.* J. Lipid Res. **49:** 1794–1806.

Sutoh, K., Sanuki, N., Sakaki, T., and Imai, R. (2010). Specific induction of TaAAPT1, an ER- and Golgi-localized ECPT-type aminoalcoholphosphotransferase, results in preferential accumulation of the phosphatidylethanolamine membrane phospholipid during cold acclimation in wheat. Plant Mol. Biol. **72:** 519–531.

Tabuchi, T., Okada, T., Azuma, T., Nanmori, T., and Yasuda, T. (2006). Posttranscriptional regulation by the upstream open reading frame of the phosphoethanolamine N-methyltransferase gene. Biosci. Biotechnol. Biochem. **70:** 2330–2334.

Testerink, C., and Munnik, T. (2011). Molecular, cellular, and physiological responses to phosphatidic acid formation in plants. J. Exp. Bot. **62:** 2349–2361.

Vance, J.E. (2008). Phosphatidylserine and phosphatidylethanolamine in mammalian cells: two metabolically related aminophospholipids. J. Lipid Res. **49:** 1377–1387.

van den Brink-van der Laan, E., Killian, J.A., and de Kruijff, B. (2004). Nonbilayer lipids affect peripheral and integral membrane proteins via changes in the lateral pressure profile. Biochim. Biophys. Acta **1666:** 275–288.

Wang, X., Devaiah, S.P., Zhang, W., and Welti, R. (2006). Signaling functions of phosphatidic acid. Prog. Lipid Res. **45:** 250–278.

Wang, Z., and Benning, C. (2012). Chloroplast lipid synthesis and lipid trafficking through ER-plastid membrane contact sites. Biochem. Soc. Trans. **40:** 457–463.

Welti, R., Li, W., Li, M., Sang, Y., Biesiada, H., Zhou, H.E., Rajashekar, C.B., Williams, T.D., and Wang, X. (2002). Profiling membrane lipids in plant stress responses. Role of phospholipase D alpha in freezing-induced lipid changes in *Arabidopsis.* J. Biol. Chem. **277:** 31994–32002.

Wilkinson, E.J., Twell, D., and Lindsey, K. (1997). Activities of CaMV 35S and nos promoters in pollen: Implications for field release of transgenic plants. J. Exp. Bot. **48:** 265–275.

Williams, J.P., Khan, M.U., and Wong, D. (1995). A simple technique for the analysis of positional distribution of fatty acids on di- and triacylglycerols using lipase and phospholipase A2. J. Lipid Res. **36:** 1407–1412.

Yadegari, R., and Drews, G.N. (2004). Female gametophyte development. Plant Cell **16** (suppl.): S133–S141.

Yamaoka, Y., Yu, Y., Mizoi, J., Fujiki, Y., Saito, K., Nishijima, M., Lee, Y., and Nishida, I. (2011). PHOSPHATIDYLSERINE SYNTHASE1 is required for microspore development in *Arabidopsis thaliana.* Plant J. **67:** 648–661.